Appendix

Quartz-in-garnet inclusion barometry under fire: Reducing uncertainty from model estimates

Kyle T. Ashley, Matthew Steele-MacInnis, Robert J. Bodnar, and Robert S. Darling

ANALYTICAL METHODS

Unpolarized Raman spectra of quartz were obtained on a JY Horiba LabRAM HR800 Raman microprobe at Virginia Tech, using a high-resolution 800 mm focal-length spectrometer with 1800 lines/mm grating and a 100mW 514.57 nm argon laser. We used a 40x objective with a confocal aperture of 400 and a 150 µm slit width. The spectra were centered at 360 cm^{-1} (range of 73.8–633.1 cm^{-1}) to allow simultaneous collection of the three main quartz peaks (~464, 206 and 127 cm^{-1} at ambient conditions) and three Ar plasma lines (520.30, 266.29 and 116.04 cm^{-1}), for drift correction. The Sifnos sample was analyzed using a 600 lines/mm grating (spectral range of 90.8–1909.7 cm^{-1}, centered at 1000 cm^{-1}), with a Hg calibration lamp (1122.58 cm^{-1}) for drift correction. Analyses included a 30 s dwell time over three acquisitions. All Raman lines were fitted using Peakfit v4.12 from SYSTAT Software Inc., using the Pearson IV model (as described for quartz by Schmidt and Ziemann, 2000; Schmidt et al., 2013). A linear drift correction was applied to the peak positions based on the observed drift on the reference Ar plasma lines. Replicate analyses of a quartz standard were conducted periodically over one week, with the weighted average 464 cm^{-1} mode (ν_{464}) ambient position at 464.546 ± 0.052 cm^{-1} (2σ; Fig. DR1), suggesting uncertainty in measured peak positions is less than ±0.1 cm^{-1}. Inclusion pressure was calculated from measured waveshifts using the equation from Ashley et al. (2014), based on the dataset of Schmidt and Ziemann (2010):

$$P\ (bar) = 4.204(\pm 0.81) \cdot \Delta\nu^2 + 1094.5(\pm 12) \cdot \Delta\nu$$

ADDITIONAL COMPUTATIONAL CONSIDERATIONS AND METHODS

Using the room temperature shear modulus for garnet to interpret results of experiments conducted at elevated temperatures may introduce offset between the modeled and measured P_{incl} trends. However, the temperature derivatives of the garnet shear moduli are relatively small (~10 MPa/K; Soga, 1967) and would only introduce errors in the calculated P_{incl} of ~1 MPa with 300 °C of heating. This also suggests that experimental uncertainty in the value of the garnet shear modulus (92.1 GPa; Wang and Ji, 2001) has a negligible effect on the calculated P_{incl} in this study.

Inclusion pressure is determined for each garnet endmember where Al occupies the Y-crystallographic site (almandine, spessartine, pyrope and grossular; shaded fields in Fig. 2B); P_{incl} is calculated for the specific composition of each garnet using an ideal linear mixing model between the garnet end-members (dashed lines in Fig. 2B), according to published garnet chemical data (see reference reported for each sample). Molar volumes of quartz and garnet were calculated in Frendly, a subsidiary program within Perple_X (Connolly, 2009), using the modified Tait *P-V-T* equation of state of Holland and Powell (2011). The shear moduli of garnet endmembers are from Wang and Ji (2001).

The pressure in the host mineral is assumed to rise from ambient (1 bar) at the surface of the grain and increase to the inclusion pressure at the inclusion/host interface. As discussed in the main text, thick sections were prepared to 100–200 μm to ensure no stress relaxation of the inclusion occurred (i.e., pressure in the garnet host is ~1 bar at the planes of the thick section with respect to the analyzed inclusion).

REFERENCES CITED

Ashley, K. T., Caddick, M. J., Steele-MacInnis, M., Bodnar, R. J., and Dragovic, B., 2014, Geothermobarometric history of subduction recorded by quartz inclusions in garnet: Geochemistry Geophysics Geosystems, v. 15, no. 2, p. 350-360.

Connolly, J. A. D., 2009, The geodynamic equation of state: What and how: Geochemistry Geophysics Geosystems, v. 10, no. 10, p. 1-19.

Holland, T., and Powell, R., 2011, An improved and extended internally consistent thermodynamic dataset for phases of petrological interest, involving a new equation of state for solids: Journal of Metamorphic Geology, v. 29, p. 333-383.

Schmidt, C., Steele-MacInnis, M., Watenphul, A., and Wilke, M., 2013, Calibration of zircon as a Raman spectroscopic pressure sensor to high temperatures and application to water-silicate melt systems: American Mineralogist, v. 98, no. 4, p. 643-650.

Schmidt, C., and Ziemann, M. A., 2000, In-situ Raman spectroscopy of quartz: A pressure sensor for hydrothermal diamond-anvil cell experiments at elevated temperatures: American Mineralogist, v. 85, p. 1,725-721,734.

Soga, N., 1967, Elastic constants of garnet under pressure and temperature: Journal of Geophysical Research, v. 72, no. 16, p. 4227-4234.

Wang, Z., and Ji, S., 2001, Elasticity of six polycrystalline silicate garnets at pressure up to 3.0 GPa: American Mineralogist, v. 86, p. 1209-1218.

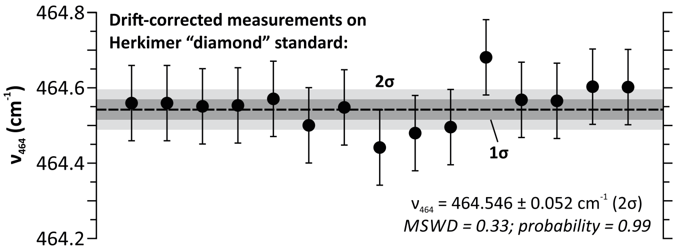

Figure DR1 Drift-corrected measurements of the n_{464} Raman band of a quartz standard from Herkimer, New York, USA, over a period of one week.

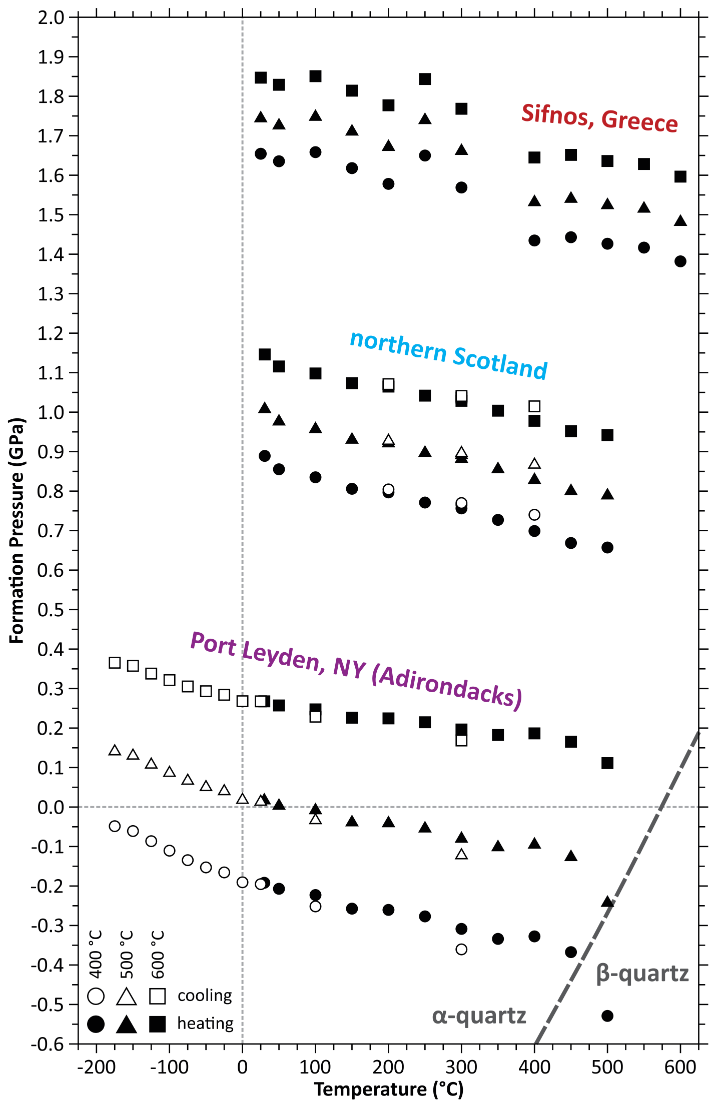

Figure DR2 Calculated formation pressures for each temperature step during experiments.

Table DR1. Frequency shift of quartz inclusions in garnet with heating

		$\Delta\nu_{464}$ (cm^{-1})		Inclusion
	Temperature (°C)	**Measured**	**Corrected[a]**	**Pressure (MPa)**
Scotland (sample MT-09-09)	31	2.588	2.716	300
	50	2.331	2.709	300
	100	1.730	2.819	312
	150	1.037	2.895	320
	200	0.430	3.089	342
	250	-0.251	3.217	356
	300	-0.835	3.424	380
	300	-0.787	3.472	385
	350	-1.419	3.589	398
	400	-1.900	3.791	421
	450	-2.373	4.030	448
	500	-2.710	4.411	491
	400[b]	-1.690	4.000	445
	300[b]	-0.761	3.499	388
	200[b]	0.468	3.127	346
Port Leyden, New York (Adirondacks)	30	-3.978	-4.064	-438
	50	-4.010	-4.062	-438
	100	-3.891	-3.870	-417
	150	-3.890	-3.813	-411
	200	-3.591	-3.475	-375
	250	-3.345	-3.207	-347
	300	-3.146	-2.999	-324
	350	-2.822	-2.680	-290
	400	-2.184	-2.059	-224
	450	-1.753	-1.657	-180
	500	-1.851	-1.794	-195
	300[b]	-3.545	-3.398	-367
	100[b]	-4.126	-4.104	-442
	25[b]	-4.031	-4.126	-444
	0[b]	-3.959	-4.231	-456
	-25[b]	-3.837	-4.186	-451
	-50[b]	-3.803	-4.237	-456
	-75[b]	-3.716	-4.250	-458
	-100[b]	-3.584	-4.235	-456
	-125[b]	-3.433	-4.221	-454
	-150[b]	-3.267	-4.213	-454
	-175[b]	-3.203	-4.336	-467
Sifnos, Greece	25	6.670	6.722	755
	50	6.344	6.722	755
	100	5.930	7.010	788
	150	5.161	7.019	789
	200	4.366	7.025	790
	250	4.097	7.565	852
	300	3.157	7.417	835
	400	1.630	7.320	824
	450	1.255	7.658	863
	500	0.797	7.917	893
	550	0.405	8.244	931
	600	-0.047	8.510	962

[a] *Frequency shift corrected for heating perturbations (i.e., shift attributed to inclusion pressurization)*

[b] *Measurements made during experimental cooling*